

MACROCELL MULTIPLE-INPUT MULTIPLE-OUTPUT SYSTEM WITH LOCAL-TO-MOBILE AND LOCAL-TO-BASE SCATTERERS

Gang Shi and Arye Nehorai

Department of Electrical and Computer Engineering at
The University of Illinois at Chicago
Chicago, IL 60607

ABSTRACT

We develop a semi-deterministic semi-stochastic channel model for the multiple-input multiple-output (MIMO) system under the macrocell environment with local-to-mobile and local-to-base scatterers, and show that the channel capacity, multiplexing and diversity gains are *multipath limited* in the sense that they are limited by the number of multipaths around the base station. We derive a lower bound on the ergodic capacity and an upper bound on the average pairwise error detection probability. It is shown that the base-station array affects the two different information theoretic measures through the same metric, and the fading correlation matrix also appears in the two bounds with the same form. Numerical examples show the tightness of the two bounds.

1. INTRODUCTION

Multiple-input multiple-output (MIMO) systems use antenna arrays on both the transmitter and receiver sides, and have been one of the most active topics in communication research lately. A MIMO system under rich scattering environment was shown to provide much higher channel capacity compared with traditional single-input multiple-output (SIMO) systems [1], [2]. Many space-time signal processing schemes have been proposed to explore the spatial multiplexing and diversity gains provided by MIMO systems. Recently, more research work has been done to evaluate the MIMO systems under more realistic scenarios. Spatial fading correlation and its effect on the MIMO capacity are examined in [3]-[5]. Environmental issues are considered in [6]. The degenerate channel case, or keyholes, is reported in [7]. Since the widely used ideal i.i.d. Gaussian matrix channel model contains no explicit environmental parameters and physical propagation models conversely require too much information of the environment, it is necessary to find *efficient, accurate and tractable* MIMO channel models for the realistic scenarios. A more general stochastic channel model is proposed in [8] and an intermediate virtual channel representation is developed in [9]. Both of these two models have symmetric structures that model the scattering on both the transmitter and receiver sides in the same way.

In this paper, we consider a MIMO channel under a suburban or rural macrocell environment, where there are typically few scatterers surrounding the base station and rich scattering around the mobile station. In addition, the local-to-base scattering is much

more stationary than the local-to-mobile one. This configuration will finally induce a semi-deterministic semi-stochastic model.

Notation: We use bold upper letters to denote matrices; bold lower letters denote vectors; $(\cdot)^*$, $(\cdot)^T$, $(\cdot)^\dagger$ denote conjugate, transpose, and Hermitian transpose respectively; $E\{\cdot\}$ represents expectation; $\text{tr}\{\cdot\}$ trace of a matrix; \mathbf{I}_n denotes the identity matrix of size n ; \otimes represents the Kronecker product; $\text{vec}(\cdot)$ stacks the first to the last columns of the matrix one under another to form a long vector; $\|\cdot\|_F$ represents the Frobenius norm of a matrix; $\exp(\cdot)$, $\log(\cdot)$ stand for the exponential function and natural logarithm function respectively; a circularly symmetric complex Gaussian random variable z is a random variable $z = x + jy$, where x and y are independent Gaussian random variable with equal variances; χ_n^2 represents a Chi-square distributed random variable with n degrees of freedom.

2. CHANNEL MODEL

We consider the uplink channel of a wireless communication system with b element antenna array at the base station, m elements at the mobile station and L local-to-base scatterers. We treat the local-to-base scatterers as receivers and transmitters which re-transmit the received signals by multiplying the scattering coefficients and neglect multiple scattering among them. Firstly, we model the channel from the mobile station to the local-to-base scatterers. Since the local-to-mobile scatterers are usually not far away from the mobile station, we further assume that the multipath spread induced by the local-to-mobile scatterers is small than the inverse of the signal bandwidth B , then the channel experiences a frequency flat fading. We also assume that the symbol period is much smaller than the channel coherence time and apply the slow blocking fading for the analysis tractable purpose. Under the macrocell environment, scatterers surrounding the mobile station are about the same height as or are higher than the mobile, thus there is always a rich scattering environment around the mobile station [10]. Assume that the mobile station antennas are separated large enough that they fade independently. Then, the channel from the m mobile station antennas to the L local-to-base scatterers can be written as \mathbf{K}^T , where $\mathbf{K} = [\mathbf{h}_1, \mathbf{h}_2 \cdots \mathbf{h}_L]$ and $\mathbf{h}_l = [h_{1,l}, \dots, h_{m,l}]^T$, $l = 1, 2, \dots, L$. The channel undergoes a Rayleigh fading if there is no dominant path in the local-to-mobile scattering or line-of-sight between the local-to-base scatterers and the mobile antennas, or a Ricean fading otherwise [10].

In this paper we will focus on the Raleigh fading case and assume the elements in \mathbf{K} are jointly circularly symmetric complex Gaussian random variables with zero means and unit variances,

This work was supported by the Air Force Office of Scientific Research Grant F49620-02-1-0339, the National Science Foundation Grants CCR-0105334 and CCR-0330342, and the Office of Naval Research Grant N00014-01-1-0681.

and $h_{1,l}, \dots, h_{m,l}$ are independent for any $1 \leq l \leq L$. However, $h_{j,1}, \dots, h_{j,L}$ might be correlated, for any $1 \leq j \leq m$, which depends on the spacing between the local-to-base scatterers, distances from the local-to-base scatterers to the mobile station and the assumption of the local-to-mobile scatterers distribution. Several distributions can be considered, including uniform, Gaussian and Laplacian [8]. Assume that the receive fading correlations between two local-to-base scatterers are the same for every mobile antenna, the covariance matrix of \mathbf{K}^T has the Kronecker structure as $\mathbf{E}\{\text{vec}(\mathbf{K}^T)\text{vec}(\mathbf{K}^T)^\dagger\} = \mathbf{I}_m \otimes \boldsymbol{\Sigma}$ and $\mathbf{E}\{\mathbf{K}^T \mathbf{K}^*\} = m\boldsymbol{\Sigma}$.

Without the local-to-base scatterers, large antenna separations are required to achieve the independent fading at the base-station antennas under the macrocell environment, making the size of the antenna array an issue. In this paper, instead of assuming large separation among the base-station antennas, we consider closely-spaced antennas, e.g., a uniform linear array (ULA) with half wavelength spacing. Signals are transmitted from the mobile antennas via local-to-mobile scatterers to the local-to-base scatterers, and then scattered to the base-station array. Here, we assume narrow-band plane waves impinging on the base-station antennas, the channel from the local-to-base scatterers to the base-station array is a line-of-sight deterministic channel, given by $\mathbf{A} = [\alpha_1 \mathbf{a}(\theta_1), \alpha_2 \mathbf{a}(\theta_2) \cdots \alpha_L \mathbf{a}(\theta_L)]$, α_l and θ_l are the scattering coefficient and angle of arrival (AOA) of the l -th local-to-base scatterer respectively, $\mathbf{a}(\theta_l) = [a_1(\theta_l), a_2(\theta_l), \dots, a_b(\theta_l)]^T$ is the so-called array response vector or steering vector [11]. Note that $\mathbf{a}(\theta_l)$ is a function of the array configuration, carrier frequency and AOA, which affect the phase difference of the signals received at each antenna with respect to the reference point.

The uplink MIMO channel model can then be written as

$$\mathbf{H} = \mathbf{A}\mathbf{K}^T. \quad (2.1)$$

From (2.1) we can see that the channel model has an asymmetric structure that the array configuration and environmental parameters of the base station are included in the model explicitly but not for the mobile station.

3. MAIN RESULTS

Based on the channel model (2.1), we can predict the performance of the MIMO system under the macrocell environment. Since the number of local-to-base scatterers is typically few, we assume $L \leq \min\{m, b\}$ in the rest of this paper. The maximum multiplexing gain and the achieving conditions are given as followed.

Theorem 1: The maximum multiplexing gain is L and, it is achieved if and only if both \mathbf{A} and \mathbf{K} have a rank of L .

Proof: the *only if* part is obvious. The *if* part can be proved straightforwardly as follows. Since \mathbf{A} is of full-column rank, any vector \mathbf{x} satisfying $\mathbf{H}\mathbf{x} = \mathbf{A}\mathbf{K}^T\mathbf{x} = \mathbf{0}$ also satisfies $\mathbf{K}^T\mathbf{x} = \mathbf{0}$. And because \mathbf{K} is of full-column rank with probability 1, the rank of the null space of \mathbf{K}^T is $m - L$ with probability 1, thus the rank of the null space of \mathbf{H} is also $m - L$, which is equivalent to saying that \mathbf{H} is of rank L . Here, we refer to the rank as the complex rank. \square

We can see from the above that the number of available sub-channels is limited by the number of multipaths around the base station, the local-to-base scatterers help build the rank of the channel matrix. The full-column rank \mathbf{A} requires that $\mathbf{a}(\theta_1), \mathbf{a}(\theta_2) \cdots \mathbf{a}(\theta_L)$, the array responses to the local-to-base scatterers, are linearly independent. And the full-column rank \mathbf{K} with probability one requires that $\mathbf{h}_1, \mathbf{h}_2 \cdots \mathbf{h}_L$ not be fully correlated.

We assume that the transmitter has no channel state information (CSI) and the receiver knows the channel perfectly. The average total input power at the transmitter side is P and the random noise at each receiver antenna is independent additive circularly symmetric complex Gaussian noise with zero-mean and variance σ^2 . The ‘‘capacity’’ is referred to as ‘‘ergodic capacity’’ in this paper.

Theorem 2: The capacity of the MIMO system (2.1) with rank L is

$$C = \mathbf{E}\{\log \det(\mathbf{I}_L + \frac{P}{m\sigma^2} \mathbf{A}^\dagger \mathbf{A} \mathbf{K}^T \mathbf{K}^*)\} \quad (3.1)$$

and a lower bound is

$$C_{\text{lb}} = L \log\left(\frac{P}{m\sigma^2}\right) + \log \det(\mathbf{A}^\dagger \mathbf{A}) + \log \det(\boldsymbol{\Sigma}) + \sum_{l=1}^L \psi(m - l + 1), \quad (3.2)$$

where $\psi(x)$ is the *digamma* function [12].

Proof: See the Appendix. \square

The lower bound (3.2) is tight for high signal-to-noise ratio (SNR) and that the capacity increases by L nats/sec/Hz for every 3 dB increase of the SNR. We say that the capacity is *multipath limited* in the sense that it grows linearly with L , instead of $\min(b, m)$, when the SNR is large. The base-station antenna array affects the lower bound (3.2) through $\det(\mathbf{A}^\dagger \mathbf{A})$ and the fading correlation by $\det(\boldsymbol{\Sigma})$.

Besides the channel capacity, the error exponent is another important information-theoretic measure, since it sets ultimate bounds on the performance of communications systems employing codes of finite memory. Suppose that $\mathbf{X}^{(i)}$ is the transmitted $m \times N$ codeword, where N is the block length and $N \geq m$. We assume that the code book is constructed satisfying the rank criterion for Rayleigh space-time codes [14], i.e., $\mathbf{X}^{(i)} - \mathbf{X}^{(j)}$ is full rank for any pair of codewords in the code book. Suppose a maximum-likelihood (ML) rule is employed to detect each codeword. Then the Chernoff bound and an upper bound of the average pairwise error probability of deciding on the codeword $\mathbf{X}^{(j)}$ instead of $\mathbf{X}^{(i)}$, where $j \neq i$, is given as follows.

Theorem 3: The pairwise error probability (PEP) averaged over channel realizations of the MIMO system (2.1) with rank L is bounded as

$$P_e < \det^{-1}(\mathbf{I}_{mL} + \frac{1}{4\sigma^2} [(\mathbf{X}^{(i)} - \mathbf{X}^{(j)})^* (\mathbf{X}^{(i)} - \mathbf{X}^{(j)})^T]) \otimes [\mathbf{A}^\dagger \mathbf{A} \boldsymbol{\Sigma}] \quad (3.3)$$

$$< (4\sigma^2)^{mL} \det^{-L}((\mathbf{X}^{(i)} - \mathbf{X}^{(j)})^* (\mathbf{X}^{(i)} - \mathbf{X}^{(j)})^T) \det^{-m}(\mathbf{A}^\dagger \mathbf{A}) \det^{-m}(\boldsymbol{\Sigma}). \quad (3.4)$$

Proof: See the Appendix. \square

The upper bound (3.4) approaches the Chernoff upper bound (3.3) when the SNR is large and it provides more insights into the relationship between the system parameters and the error probability. From (3.4) we can see that the upper bound of the average pairwise error probability is a function of $(\sigma^2)^{mL}$, thus the system has a diversity gain of mL . So the diversity gain is also *multipath limited* in the sense that it is linear to the number of multipaths around the base station.

From (3.2) and (3.4), we find that the base-station array configuration affects both the lower bound of the channel capacity and the upper bound of the average pairwise error probability by $\det(\mathbf{A}^\dagger \mathbf{A})$. Therefore, maximizing $\det(\mathbf{A}^\dagger \mathbf{A})$ when designing the

base-station array, the two different information theoretic measures are optimized simultaneously. The same is also true for the fading correlation matrix Σ , which affects the two bounds through $\det(\Sigma)$.

Recalling the MIMO channel (2.1), it can be interpreted as two cascaded MIMO systems: \mathbf{K}^T represents the first $L \times m$ MIMO system from the mobile station to the local-to-base scatterers, which is stochastic with independent columns and correlated rows, and \mathbf{A} represents the second $b \times L$ MIMO system from the local-to-base scatterers to the base-station antennas, which is a deterministic “line-of-sight” model. The local-to-base scatterers not only help the system build rank of the channel matrix, but also increase the effective aperture of the base-station array; they obtain the spatial diversity, which is further explored by the base-station antenna array as the angle diversity. It is the local-to-base scatterers that help the system achieve the diversity without requiring large physical size of the base-station array.

4. NUMERICAL EXAMPLES

In this section, we provide simulation examples demonstrating our analytical results. We adopt Lee’s model [10] to calculate the fading correlation matrix Σ . Assume the coordinates origin is at the reference point of the base-station array and the mobile station is at (3000, 0) with units of wavelengths, which is about 1.125 kilometers from the base station for the 800MHz carrier frequency. Ten local-to-mobile scatterers are uniformly distributed on the circle with radius 150 wavelengths. Half-wavelength spaced ULA with 4 elements is deployed at the base station and is orientated to the x-axis with the angle of $\pi/6$. The coordinates of the two local-to-base scatterers are (141, 141), (130, -75) respectively. In the first example, we illustrate the channel capacity (3.1) and its lower bound (3.2). From Figure 1, we can see that the lower bound becomes tight when SNR is large. Here, the capacity is evaluated by Nats per second per Hertz.

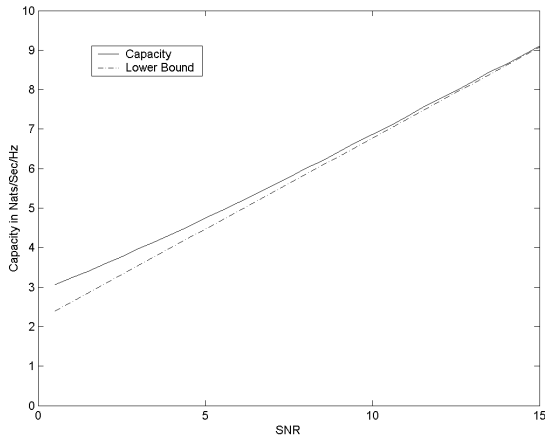


Fig. 1. Channel capacity and its lower bound.

In the second example, we show the average pairwise error detection probability and its Chernoff and upper bounds. From Figure 2, we can see that the upper bound approaches the Chernoff bound when SNR becomes large.

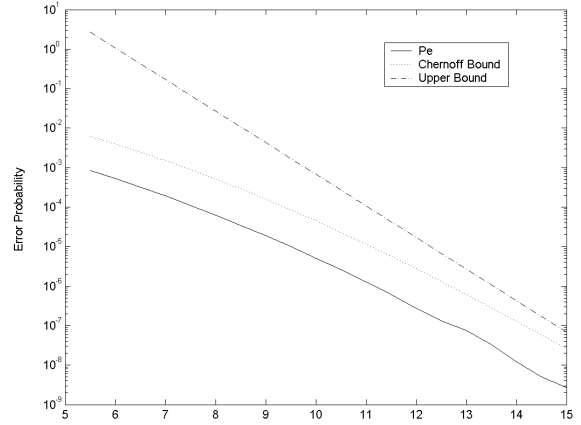


Fig. 2. Pairwise error probability and its Chernoff and upper bounds.

5. CONCLUSIONS

We developed a channel model of MIMO system under the macrocell environment with local-to-mobile and local-to-base scatterers. Our analysis of the capacity and pairwise error probability showed that the multiplexing gain, capacity, and diversity gain are limited by the number of multipaths around the base station. The base-station antenna array affects both the lower bound of the capacity and the upper bound of the error detection probability by $\det(\mathbf{A}^\dagger \mathbf{A})$ and the fading correlation through $\det(\Sigma)$. Future work will include evaluating the outage capacity, developing methods to improve the macrocell MIMO system performance and considering the scenario with remote scattering.

6. APPENDIX

In the appendix, we give the proofs of the Theorem 2 and 3.

Proof of Theorem 2:

$$\begin{aligned}
 C &= \mathbb{E}\{\log \det(\mathbf{I}_b + \frac{P}{m\sigma^2} \mathbf{H}\mathbf{H}^\dagger)\} \\
 &= \mathbb{E}\{\log \det(\mathbf{I}_b + \frac{P}{m\sigma^2} \mathbf{A}\mathbf{K}^T \mathbf{K}^* \mathbf{A}^\dagger)\} \\
 &= \mathbb{E}\{\log \det(\mathbf{I}_L + \frac{P}{m\sigma^2} \mathbf{A}^\dagger \mathbf{A} \mathbf{K}^T \mathbf{K}^*)\} \\
 &> \mathbb{E}\{\log \det(\frac{P}{m\sigma^2} \mathbf{A}^\dagger \mathbf{A} \mathbf{K}^T \mathbf{K}^*)\} \\
 &= L \log(\frac{P}{m\sigma^2}) + \log \det(\mathbf{A}^\dagger \mathbf{A}) + \mathbb{E}\{\log \det(\mathbf{K}^T \mathbf{K}^*)\} \\
 &= L \log(\frac{P}{m\sigma^2}) + \log \det(\mathbf{A}^\dagger \mathbf{A}) + \log \det(\Sigma) + \\
 &\quad \sum_{l=1}^L \psi(m-l+1),
 \end{aligned}$$

where the third equality follows from the determinant identity $\det(\mathbf{I}_m + \mathbf{A}\mathbf{B}) = \det(\mathbf{I}_n + \mathbf{B}\mathbf{A})$, where \mathbf{A} and \mathbf{B} are $m \times n$ and $n \times m$ matrices respectively, and the last equality is inferred from the fact that $2^m \det(\mathbf{K}^T \mathbf{K}^*) / \det(\Sigma)$ is distributed as is the product of L

independent χ^2 random variables with $2m, 2(m-1), \dots, 2(m-L+1)$ degrees of freedom respectively [13] and $E\{\log \chi_{2n}^2\} = \log 2 + \psi(n)$ [12]. \square

Proof of Theorem 3:

$$\begin{aligned}
P_e &= E\left\{Q\left(\sqrt{\frac{\|\mathbf{H}(\mathbf{X}^{(i)} - \mathbf{X}^{(j)})\|_F^2}{2\sigma^2}}\right)\right\} \\
&\leq E\left\{\exp\left(-\frac{\|\mathbf{H}(\mathbf{X}^{(i)} - \mathbf{X}^{(j)})\|_F^2}{4\sigma^2}\right)\right\} \\
&= E\left\{\exp\left(-\frac{\|[(\mathbf{X}^{(i)} - \mathbf{X}^{(j)})^T \otimes \mathbf{I}_b] \text{vec}(\mathbf{H})\|_F^2}{4\sigma^2}\right)\right\} \\
&= E\left\{\exp\left(-\frac{\|[(\mathbf{X}^{(i)} - \mathbf{X}^{(j)})^T \otimes \mathbf{I}_b][\mathbf{I}_m \otimes \mathbf{A}] \text{vec}(\mathbf{K}^T)\|_F^2}{4\sigma^2}\right)\right\} \\
&= E\left\{\exp\left(-\frac{\|[(\mathbf{X}^{(i)} - \mathbf{X}^{(j)})^T \otimes \mathbf{A}] \text{vec}(\mathbf{K}^T)\|_F^2}{4\sigma^2}\right)\right\} \\
&= \det^{-1}\left(\mathbf{I}_{bN} + \frac{1}{4\sigma^2}[(\mathbf{X}^{(i)} - \mathbf{X}^{(j)})^T \otimes \mathbf{A}][\mathbf{I}_m \otimes \boldsymbol{\Sigma}]\right. \\
&\quad \left. [(\mathbf{X}^{(i)} - \mathbf{X}^{(j)})^T \otimes \mathbf{A}]^\dagger\right) \\
&= \det^{-1}\left(\mathbf{I}_{bN} + \frac{1}{4\sigma^2}[(\mathbf{X}^{(i)} - \mathbf{X}^{(j)})^T (\mathbf{X}^{(i)} - \mathbf{X}^{(j)})^*] \otimes [\mathbf{A}\boldsymbol{\Sigma}\mathbf{A}^\dagger]\right) \\
&= \det^{-1}\left(\mathbf{I}_{mL} + \frac{1}{4\sigma^2}[(\mathbf{X}^{(i)} - \mathbf{X}^{(j)})^* (\mathbf{X}^{(i)} - \mathbf{X}^{(j)})^T] \otimes [\mathbf{A}^\dagger \mathbf{A}\boldsymbol{\Sigma}]\right) \\
&< (4\sigma^2)^{mL} \det^{-L}((\mathbf{X}^{(i)} - \mathbf{X}^{(j)})^* (\mathbf{X}^{(i)} - \mathbf{X}^{(j)})^T) \\
&\quad \det^{-m}(\mathbf{A}^\dagger \mathbf{A}) \det^{-m}(\boldsymbol{\Sigma}),
\end{aligned}$$

where the fifth identity can be derived following similar procedures at [15] and the seventh equality comes from the Lemma 1, which is a generalization of matrix determinant identity $\det(\mathbf{I}_m + \mathbf{A}\mathbf{B}) = \det(\mathbf{I}_n + \mathbf{B}\mathbf{A})$. \square

Lemma 1:

$$\begin{aligned}
&\det(\mathbf{I}_{mr} + \mathbf{A}\mathbf{B} \otimes \mathbf{C}\mathbf{D}) \\
&= \det(\mathbf{I}_{mr} + \mathbf{C}\mathbf{D} \otimes \mathbf{A}\mathbf{B}) \\
&= \det(\mathbf{I}_{nr} + \mathbf{B}\mathbf{A} \otimes \mathbf{C}\mathbf{D}) \\
&= \det(\mathbf{I}_{ms} + \mathbf{A}\mathbf{B} \otimes \mathbf{D}\mathbf{C}),
\end{aligned}$$

where $\mathbf{A}, \mathbf{B}, \mathbf{C}$ and \mathbf{D} are $m \times n, n \times m, r \times s$ and $s \times r$ matrices respectively.

Proof: Suppose $\lambda_1, \lambda_2, \dots, \lambda_m$ are the eigenvalues of $\mathbf{A}\mathbf{B}$ including repeated and zero eigenvalues, and $\mu_1, \mu_2, \dots, \mu_r$ are eigenvalues of $\mathbf{C}\mathbf{D}$. Then $\lambda_i \mu_j, i = 1, 2, \dots, m, j = 1, 2, \dots, r$ are eigenvalues of $\mathbf{A}\mathbf{B} \otimes \mathbf{C}\mathbf{D}$ [16]. The first equality follows directly from the following identity.

$$\det(\mathbf{I}_{mr} + \mathbf{A}\mathbf{B} \otimes \mathbf{C}\mathbf{D}) = \prod_{i=1}^m \prod_{j=1}^r (1 + \lambda_i \mu_j).$$

The second and third equalities follows from above identity and the fact that $\mathbf{A}\mathbf{B}$ and $\mathbf{C}\mathbf{D}$ have the same nonzero eigenvalues as $\mathbf{B}\mathbf{A}$ and $\mathbf{D}\mathbf{C}$ respectively. \square

7. ACKNOWLEDGMENTS

The authors would like to thank Bert Hochwald of Bell Labs and Erik G. Larsson of George Washington University for their helpful comments.

8. REFERENCES

- [1] G. J. Foschini and M. J. Gans, "On limits of wireless communications in a fading environment when using multiple antennas," *Wireless Personal Commun.*, vol. 6, pp. 311-335, Mar. 1998.
- [2] I. E. Telatar, "Capacity of multi-antenna Gaussian channels," *European Trans. Telecommun.*, vol. 10, no. 6, pp. 585-595, Nov. 1999.
- [3] D. Shiu, G. J. Foschini, M. J. Gans, J. M. Kahn, "Fading correlation and its effect on the capacity of multielement antenna systems," *IEEE Trans. Commun.*, vol. 48, issue 3, pp. 502-513, Mar. 2000.
- [4] C. Chuah, D. N. C. Tse, J. M. Kahn and R. A. Valenzuela, "Capacity scaling in MIMO wireless systems under correlated fading," *IEEE Trans. Inform. Theory*, vol. 48, issue 3, pp. 637-650, Mar. 2002.
- [5] S. L. Loyka, "Channel capacity of MIMO architecture using the exponential correlation matrix," *IEEE Commun. Lett.*, vol. 5, issue 9, pp. 369-371, Sep. 2001.
- [6] D. W. Bliss, K. W. Forsythe, A. O. Hero III, and A. F. Yegulalp, "Environmental issues for MIMO capacity," *IEEE Trans. Signal Processing*, vol. 50, issue 9, pp. 2128-2142, Sep. 2002.
- [7] D. Chizhik, G. J. Foschini, M. J. Gans and R. A. Valenzuela, "Keyholes, correlations, and capacities of multielement transmit and receive antennas," *IEEE Trans. Wireless Commun.*, vol. 1, issue 2, pp. 361-368, Apr. 2002.
- [8] D. Gesbert, H. Bölcskei, D. A. Gore, and A. J. Paulraj, "Outdoor MIMO wireless channels: models and performance prediction," *IEEE Trans. Commun.*, vol 50, issue 12, pp. 1926-1934, Dec. 2002.
- [9] A. M. Sayeed, "Deconstructing multiantenna fading channels," *IEEE Trans. Signal Processing*, vol. 50, issue 10, pp. 2563-2579, Oct. 2002.
- [10] R. B. Ertel, P. Cardieri, K. W. Sowerby, T. S. Rappaport, and J. H. Reed, "Overview of spatial channel models for antenna array communication systems," *IEEE Personal Commun.*, vol. 5, issue 1, pp. 10-22, Feb. 1998.
- [11] A. Paulraj and C. B. Papadias, "Space-time processing for wireless communications," *IEEE Signal Processing Magazine*, vol. 14, pp. 49-83, Nov. 1997.
- [12] O. Oyman, R. U. Nabar, H. Bölcskei, A. J. Paulraj, "Characterizing the Statistical Properties of Mutual Information in MIMO Channels," *IEEE Trans. Signal Processing*, vol. 51, issue 11, pp. 2060-2126, Nov. 2003.
- [13] N. R. Goodman, "The distribution of the determinant of a complex Wishart distributed matrix," *Ann. Math. Stat.*, vol. 34, no. 1, pp. 178-180, Mar. 1963.
- [14] V. Tarokh, N. Seshadri, A. R. Calderbank, "Space-time codes for high data rate wireless communication: performance criterion and code construction," *IEEE Trans. Inform. Theory*, vol. 44, issue 2, pp. 744-765 Mar. 1998.
- [15] E. G. Larsson, P. Stoica, *Space-Time Block Coding for Wireless Communications*, Cambridge University Press, 2003.
- [16] J. W. Brewer, "Kronecker products and matrix calculus in system theory," *IEEE Trans. Circuits and Systems*, vol. cas-25, no. 9, pp. 772-781, Sep. 1978.